Sixth International Symposium on Marine Propulsors
smp'19, Rome, Italy, May 2019

Propeller Optimization for a single screw ship using BEM supported by cavitating CFD

Simon Törnros, Olof Klerebrant, Emrah Korkmaz, Tobias Huuva

Caterpillar Propulsion, Öckerö, Sweden

ABSTRACT

A propeller is optimized for a 90 m multi-purpose vessel using a competitive multi-objective particle swarm optimization algorithm. The optimization is setup with three goals: maximize efficiency, minimize pressure pulses and minimize pressure side cavitation. A Boundary Element Method software is used by the optimizer for hydrodynamic analysis. The optimization results show a generally well converged Pareto front and a wide solution set indicates that the algorithm did achieve sufficient diversity. Clear trade-offs are found between the efficiency and the 1st order pressure pulse, and between pressure side cavitation and 1st order pressure pulse. The results show that the 1st order pressure pulse can be improved by allowing more pressure side cavitation. Generally, lower efficiencies are seen for individuals with more pressure side cavitation, however all propellers with the highest efficiencies do have some pressure side cavitation. On the efficiency - 1st order pressure pulse Pareto front, the least amount of pressure side cavitation is found near the knee point. Three individuals from the optimization results are also analyzed in cavitating condition using RANS based CFD to assess efficiency and pressure pulses. The CFD results show a small and consistent difference to the results using the BEM method.

Keywords

Propeller, optimization, BEM, CFD, cavitation

1 INTRODUCTION

The optimum propeller design is a tradeoff between conflicting performance factors such as efficiency, noise and vibrations, and structural strength. Furthermore, there is also a tradeoff due to the conflict between performance in multiple operational conditions, such as high and low vessel speed.

Blade design is a time-consuming matter, where a large set of evaluations must be made at every design update. Exploring the design space for a high-end propeller design manually may require weeks of work even for an experienced blade designer, making automatic optimization potentially a vital tool in designing better propellers using less resources.

This study aims to apply an optimization method for a single screw open propeller on a multi-purpose carrier. The method will be extended to use RANS based CFD to assess efficiency and 1st order pressure pulse amplitude in cavitating condition behind the hull.

2 Test Case

The test case used in this study is a 90 m multi-purpose carrier equipped with a single screw, open controllable pitch propeller (CPP). Three operating conditions were included in the optimization; a design condition, a slow steam maneuvering condition at high propeller rotational speed and a Maximum Continuous Rating (MCR) condition. The thrust deduction factor is assumed to be 0.2, independently of propeller design.

3 Method

A propeller blade optimization framework called Propagate has been developed by MARIN and demonstrated by Huisman (2017). The framework has been further developed within the joint industry initiative Cooperative Research Ships (CRS) and the EU funded project Multi-ObjecTive design Optimization of fluid eneRgy machines (MOTOR).

Propagate is written in MATLAB and was run using MATLAB R2018b. Propagate is further coupled with PlatEMO; an open source platform for multi-objective optimization (Tian et al. 2017).

An optimization algorithm called Competitive Mechanism based multi-Objective Particle Swarm Optimizer (CMOPSO) (Zhang et al. 2018) was used. In CMOPSO, a competition-based learning strategy is used for updating the particles with randomly performed pairwise competitions between particles in the current swarm. The winner particle guides the particle by updating the velocity. The optimization strategy is shown by Zhang et al. (2018) to achieve a better balance between convergence and diversity as compared to a regular Particle Swarm Optimizer (PSO).

The optimization included variation of traditional blade design parameters such as diameter, Blade Area Ratio (BAR) and control points for span-wise distributions of skew, pitch, chord and camber. The BAR was varied by scaling the chord distribution.

The camber distribution is described by a two-point Bezier spline, and camber level at upper and lower radii of the blade were varied in the optimization. Pitch, skew and

chord were parametrized by two G1-continous Bezier curves.

For the skew distribution, the maximum skew angle and the radial location where skew maximum on leading edge occurs were used as optimization parameters.

All optimization parameters including their box constraints can be seen in Table 1.

Table 1 Optimization parameters and their box constraints

Parameter	Min	Max
Diameter [m]	2.50	2.80
BAR [-]	0.45	0.65
Camber lower radii/D[-]	0.009	0.030
Camber upper radii/D [-]	0.012	0.020
Max chord radius [-]	0.65	0.80
Pitch hub unloading [-]	0.1	0.3
Max pitch radius [-]	0.50	0.80
Pitch tip unloading [-]	0.2	0.5
Max skew radius [-]	0.40	0.50
Maximum skew angle [°]	20	40

3.1 Goals

Three goals were applied in the optimization. The first goal is to maximize the ship efficiency, calculated as

$$\eta = \frac{V_s T(1-tdf)}{2\pi n Q} \qquad (1)$$

where V_s is the ship speed, T is the thrust, tdf is the thrust deduction factor, n is rotational speed and Q is torque on the propeller shaft.

The second goal is to minimize the first order harmonics of pressure fluctuations on the hull above the propeller.

The third goal is to minimize the amount of pressure side (PS) cavitation in low pitch condition. Accepting small amounts of pressure side cavitation can result in performance gains, which is why pressure side cavitation is treated as a minimization goal. When pressure minus vapor pressure on pressure side is negative, the net pressure is integrated, summed over the area and normalized to achieve a pressure side cavitation force coefficient.

3.2 Constraints

Before an individual enters the optimization, the geometry is checked so that the blades are not intersecting when pitching full ahead to full astern, that the blade root fits on the blade foot and so that the no-ice rules by DNV GL (2015) are fulfilled by adapting the thickness.

These pre-flight constraints speed up the optimization by evaluating more feasible individuals before entering more costly computations, such as cavitation simulations.

To avoid erosive cavitation, two constraints apply. The first is the cavity planform development constraint, developed within CRS, which controls that the cavity closure line is sufficiently parallel to incoming flow, reducing the risk of the re-entrant jet to impinge on the sheet cavity which could lead to erosive sheet cavitation.

The second constraint ensures that the minimum pressure downstream the leading edge suction peak is kept above vapor pressure in all conditions in order to avoid potentially erosive bubble cavitation.

The optimization framework with the same constraints was demonstrated for a Roll-on/roll-off passenger ferry by Törnros (2018). The results show that the optimization setup was able to produce a Pareto front which included a manual high-end design.

3.3 Low fidelity method

The low fidelity method utilized in the optimization is the low-order Boundary Element Method (BEM) software PROCAL v2.400, developed by CRS, see Bosschers (2006). It can be used to predict hydrodynamic performance in open water and in-behind condition using an effective wake field (which takes the effect of propeller induced velocity on the wake field into account) with and without cavitation. An iterative Kutta condition is used to target a zero-pressure difference in the blade wake.

Hull pressures are computed assuming incompressible, inviscid flow and that the hull point is sufficiently far from the propeller so that the induced velocity component variation is negligible compared to the time derivative of the potential. Influence of acoustic waves by ship and free surface are considered by multiplication of solid boundary factors in the frequency domain; a method further demonstrated by Bosschers et al. (2008).

3.4 High fidelity method

Due to the inviscid nature of the low fidelity method, incorrect conclusions about the tradeoffs may be drawn for extreme geometries in particular. A high fidelity CFD method was used in design condition for a selection of individuals from the Pareto front to conclude how more physics alter the shape of the front.

In the high fidelity method, the propeller was simulated in wetted and cavitating condition operating behind the hull using the C++ finite volume library OpenFOAM 2.3. The 3D geometry was exported using a Rhino plugin developed by MARIN. The discretization was carried out using ANSA 16.2.3 by BETA CAE, generating hybrid hexahedral-polyhedral meshes consisting of about 17M cells.

The solver is a transient multiphase solver which includes cavitation through the mass-transfer model by Sauer (2000). The turbulence model k-ω SST was used together with a damping function of the turbulent viscosity in the mixture region as proposed by Reboud (2002). All CFD computations were performed in full scale and used the all-Y^+ wall function in OpenFOAM.

10 propeller revolutions were simulated in wetted flow condition using a time step corresponding to 1° propeller rotation. This was followed by 5 propeller revolutions in cavitating condition, using 0.25° propeller rotation per time step. Neither the free surface nor heave or pitch were

included. Instead the free surface was replaced by a flat symmetry plane. The CFD simulations used the same operating condition as used in the BEM simulations. This means that the high-fidelity method used the same pitch as the low fidelity method and consequently any mismatch between the low- and high-fidelity method appears in the predicted thrust.

4 Results

The optimization method evaluated the design space and was considered finished when the Pareto front was sufficiently converged. The optimization ran for 52 generations, with 100 individuals per generation, making the number of evaluated propeller designs 5200.

Figure 1, Figure 2 and Figure 3 show the Pareto front. Since there are three goals, the Pareto front from this optimization is 3-dimensional.

The Pareto front is generally well converged, and the wide solution set indicates that the optimization algorithm did achieve sufficient diversity.

The trade-off between efficiency and 1st order pressure pulse in Figure 1 is very clear, the highest efficiencies can only be achieved by allowing high 1st order pressure pulse levels.

Figure 2 shows a clear trade-off between 1st order pressure pulse and pressure side cavitation. The lowest pressure pulses can only be achieved by allowing more pressure side cavitation. This is expected from typical designs with low pressure pulse; high camber and high tip pitch reduction reduce the pressure pulse but introduce or increase the amount of pressure side cavitation.

From Figure 1 it can be seen that some pressure side cavitation is present on all individuals on the Pareto front. The least amount of pressure side cavitation on the Pareto front is found near the knee point.

From Figure 3 it can be seen that the efficiency generally decreases with increased pressure side cavitation force. However, the individuals with the highest efficiencies, above 56%, all have some pressure side cavitation.

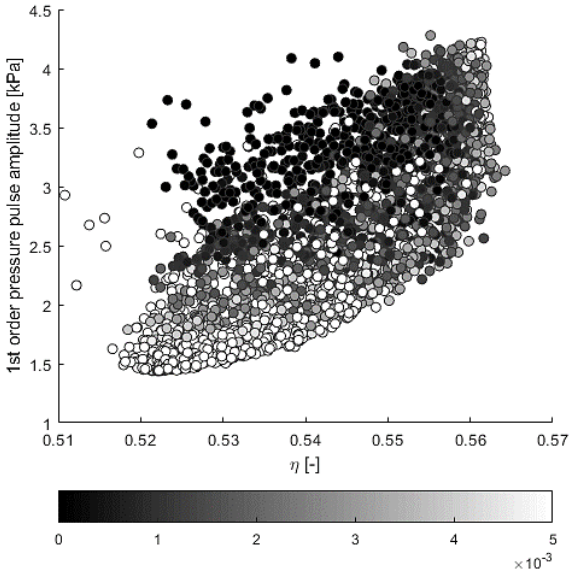

Figure 1 Efficiency and 1st order pressure pulse, colored by pressure side cavitation force coefficient

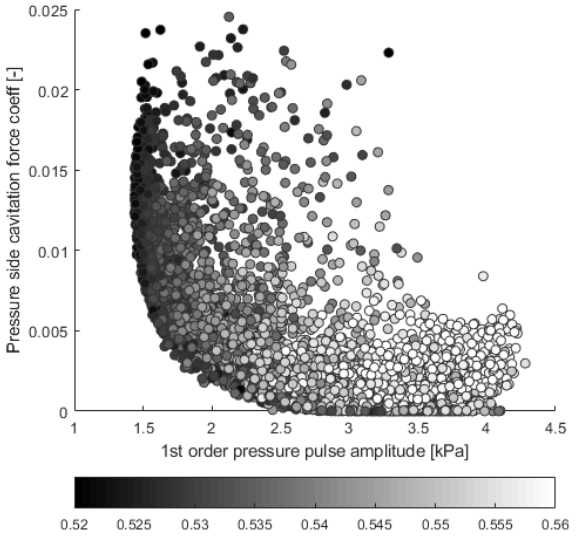

Figure 2 1st order pressure pulse and pressure side cavitation force coefficient, colored by efficiency

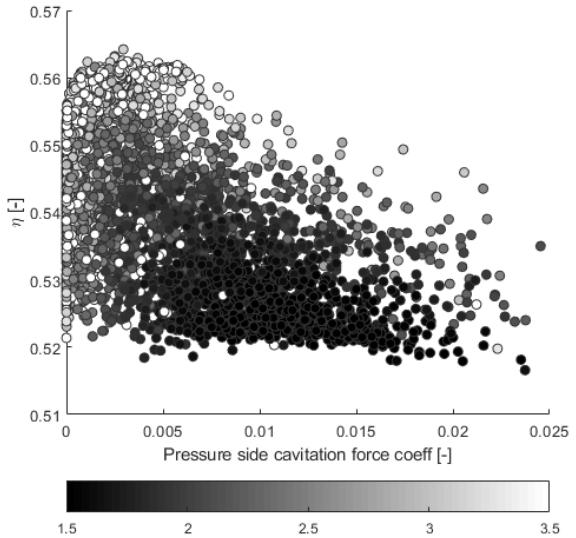

Figure 3 Pressure side cavitation force coefficient and efficiency, colored by 1st order pressure pulse

Three designs were selected for further analysis using the high-fidelity method. These three propellers were selected from extrema on the pareto front; one propeller with high efficiency (G28I69), one with low pressure pulse (G51I73) and one propeller with no pressure side cavitation in maneuvering condition (G37I95). As immediately noticeable in Figure 4, the blade designs are very different in terms of diameter, BAR and skew.

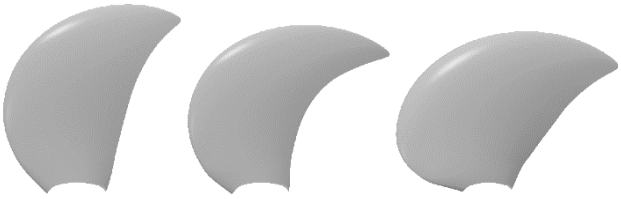

Figure 4 Selected individuals for high fidelity CFD analysis. High efficiency design (left), no pressure side cavitation design (center) and low pressure pulse design (right)

The parameter values for the three selected individuals are shown in Table 2. Values equal to a box constraint are highlighted as bold.

Table 2 Parameter values for the three selected propeller designs.

Parameter	High η design	No PS cav design	Low pulse design
Diameter [m]	2.79	2.59	**2.50**
BAR [-]	**0.45**	0.49	0.63
Camber lower/D [-]	**0.0090**	0.0100	0.0190
Camber upper/D [-]	**0.0120**	**0.0120**	0.0194
Max chord radius [-]	**0.65**	0.78	0.68
Pitch hub unloading [-]	0.27	0.29	0.12
Max pitch radius [-]	0.73	0.75	0.51
Pitch tip unloading [-]	0.26	0.39	**0.50**
Max skew radius [-]	0.42	**0.40**	**0.40**
Max skew angle [°]	28	39	**40**

The three propellers have the typical design characteristics associated with their performance. The high efficiency design has a large diameter, low blade area ratio, low camber, high pitch radial maximum, high hub pitch unloading and low tip pitch unloading, see Figure 5. This pitch distribution moves the load to the higher radii as expected for a high efficiency design. The high pitch and low camber move the load towards the leading edge, which increases the mid-chord pressure on the suction side. The increased mid-chord pressure makes the bubble cavitation constraint allow a smaller BAR, which is beneficial for the efficiency.

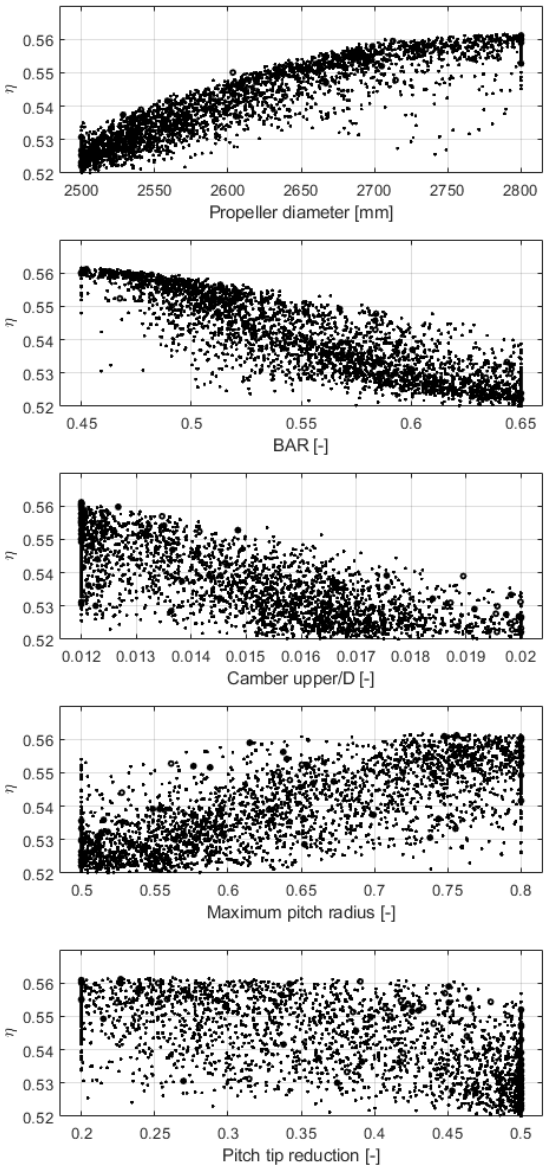

Figure 5 Parameter influence on efficiency

The design with no pressure side cavitation is similar to the high efficiency design with small BAR and little camber. The main differences are found in a smaller diameter, higher maximum chord radius, higher maximum pitch radius and higher skew. The strongest trend is found for the camber parameters, see Figure 6, which show that the camber should be decreased to achieve less pressure side cavitation, as expected.

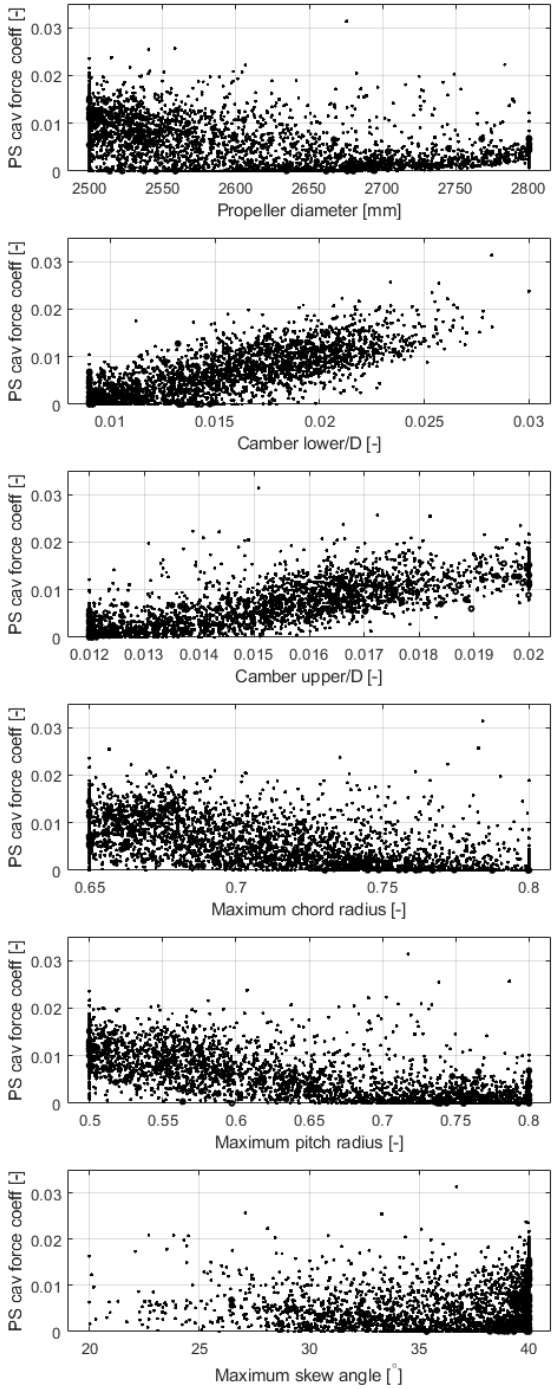

Figure 6 Parameter influence on pressure side cavitation force coefficient

The low pressure-pulse design has a small diameter, high BAR, high camber at lower and higher radii, low maximum pitch radius with little offloading at root and high offloading at tip and a high skew. The parameter influence on the pressure pulse can be seen in Figure 7. The low pulse design moves the load from the leading edge toward mid-chord, through lower pitch and higher camber compared to the high efficiency design. This means the mid-chord pressure on the suction side will be lower, so that the BAR must be increased to fulfill the bubble cavitation constraint. The low diameter of the low pulse design increases the clearance to the hull which decreases the pressure pulse further.

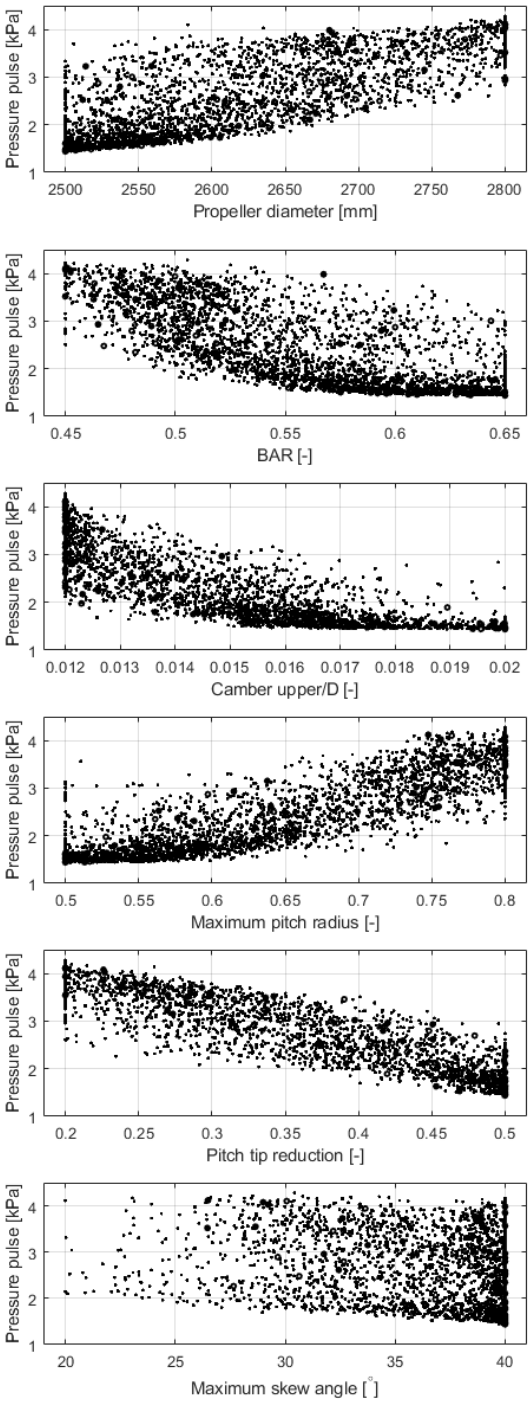

Figure 7 Parameter influence on 1st order pressure pulse amplitude

The CFD analyses are performed with the propeller behind the ship at the same pitch setting and rotational speed as in the BEM simulations in design condition. All three CFD analyses show less thrust, higher efficiency and higher first order pressure pulse amplitude in comparison with the BEM results, Table 3.

The CFD simulations predict 1.4 to 3.9 percentage lower thrust. The efficiency is found to be 1.3-1.5 percentage higher and the cavitating pressure pulse amplitude to be 0.16 to 0.34 kPa higher with CFD compared to BEM.

Table 3 Propeller performance in CFD and BEM

Code	Parameter	High η design	No PS cav design	Low pulse design
BEM	Thrust [kN]	160.5	160.5	160.5
	Power [kW]	1294	1326	1391
	Pulse [kPa]	3.72	3.09	1.45
	η [%]	56.2%	54.8%	52.2%
CFD	Thrust [kN]	157.6	154.2	158.2
	Power [kW]	1237	1243	1337
	Pulse [kPa]	4.06	3.25	1.69
	η [%]	57.7%	56.1%	53.6%

The comparison between the results using BEM and CFD shows that while there is a small mismatch in predicted thrust, efficiency and first order pressure pulse amplitude the differences are similar for all three propeller cases. This means that a Pareto front of similar shape would likely be found if the optimization relied solely on CFD.

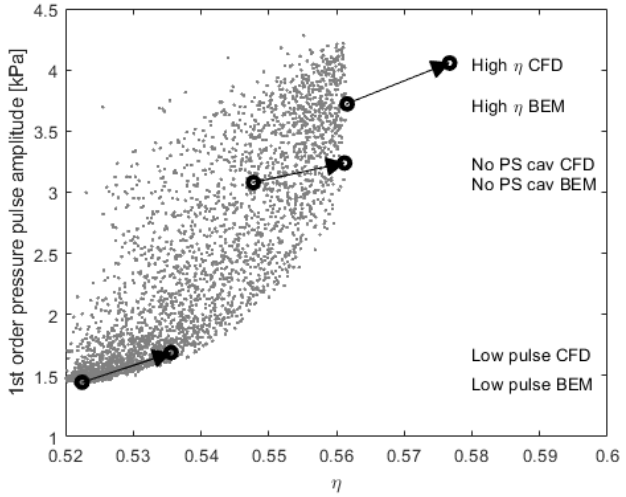

Figure 8 Pareto front from the BEM-based optimization and the predicted performance for three individuals using CFD

The comparison of cavitation on the suction side of the blades in Figure 9, Figure 10 and Figure 11 shows that there is a strong agreement between the CFD and BEM method on radial onset of cavitation. The predicted cavity extent is similar, but the CFD simulation predicts the vapor volume to peak at a later blade angle in comparison to the BEM results. Less agreement is found in the prediction of the tip vortex as PROCAL only models sheet cavitation.

Figure 9 Blade pressure and cavitation every 30°, BEM (top) and CFD (bottom) for high efficiency design

Figure 10 Blade pressure and cavitation every 30°, BEM (top) and CFD (bottom) for no pressure side cavitation design

Figure 11 Blade pressure and cavitation every 30°, BEM (top) and CFD (bottom) for low pulse design

Comparing the first 4 pressure pulse harmonics, Table 4, it can be seen that CFD predicts higher amplitudes for all 4 harmonics for all 3 propellers, except the 4th order harmonics amplitude for the low pulse design, which is higher in BEM.

Table 4 Amplitudes [kPa] for the first 4 harmonics

	Harmonics	High η design	No PS cav design	Low pulse design
BEM	1st	3.72	3.09	1.45
	2nd	1.56	0.64	0.20
	3rd	0.74	0.14	0.05
	4th	0.24	0.11	0.05
CFD	1st	4.06	3.25	1.69
	2nd	1.92	0.84	0.53
	3rd	0.86	0.34	0.26
	4th	0.52	0.30	0.03

5 Conclusion

The optimization results show a generally well converged Pareto front and a wide solution set indicates that the algorithm did achieve sufficient diversity.

Clear trade-offs are found between the efficiency and the 1st order pressure pulse, and between pressure side cavitation and 1st order pressure pulse.

The results show that the 1st order pressure pulse can be improved by allowing more pressure side cavitation. Generally lower efficiencies are seen for individuals with more pressure side cavitation, however all propeller with the highest efficiencies do have some pressure side cavitation.

On the efficiency-1st order pressure pulse Pareto front, the least amount of pressure side cavitation is found near the knee point.

The difference in predicted efficiency and cavitating pressure pulse using BEM and CFD is similar for the three studied designs. The efficiency is found to be 1.3-1.5 percentage higher with CFD, and the cavitating pressure pulse amplitude to be 0.16 to 0.34 kPa higher.

Differences of this magnitude are expected, especially since the wake fields in the two methods are different. In the BEM simulation an effective wake field is given while in CFD the wake field is part of the simulation. The consistency in the differences between CFD and BEM implies that the Pareto front achieved from the optimization using BEM is similar in shape to what would likely be found if the analyses would be performed solely using CFD.

ACKNOWLEDGEMENTS

The authors thank Evert-Jan Foeth of MARIN for providing us with the Rhino plugin used for export of the 3D geometry.

REFERENCES

Bosschers J., Vaz G., Starke A. R. & van Wijngaarden E. (2008). 'Computational analysis of propeller sheet cavitation and propeller-ship interaction'. RINA Conference (MARINE CFD2008), Southampton, UK.

DNV GL. (2015). 'Calculation of marine propellers'.

Huisman, J. Foeth, E-J. (2017). 'Automated multi-objective optimization of ship propellers'. Fifth International Symposium on Marine Propulsors. Espoo, Finland.

Reboud, J, L. Coutier-Delgosha, O. Fortes-Patella, R. (2002).'Simulation of unsteady cavitation with a two equation turbulence model including compressibility effects'. Journal of Turbulence.

Sauer, J. Schnerr, G,H. (2000). 'Unsteady Cavitating Flow – a new cavitation model based on a modified front capturing method and bubble dynamics'. Fluids Engineering Summer Conference.

Tian, Y, Cheng, R, Zhang, X, and Jin, Y. (2017). 'PlatEMO: A MATLAB platform for Evolutionary Multi-Objective Optimization [Educational forum]', IEEE Computational Intelligence Magazine, 2017, 12(4): 73-87.

Törnros, S. Klerebrant, O. (2018). 'Demonstration of Propeller Blade Optimization using BEM and CFD'. Proceedings of the 21st Numerical Towing Tank Symposium. Cortona, Italy.

Vaz G., Bosschers J. (2006). 'Modelling three dimensional sheet cavitation on marine propellers using a boundary element method'. Sixth International Symposium on Cavitation CAV2006, Wageningen, The Netherlands.

Zhang, X. Zheng, X. Cheng, R. Qiu, J. Jin, Y. (2018). 'A Competetive Mechanism Based Mult-objective Particle Swarm Optimizer with Fast Convergence'. Information Sciences 427, 63-76